Journal of Applied Polymer Science

High Tensile Strength Fiber of Poly[(*R*)-3-hydroxybutyrate-*co*-(*R*)-3-hydroxyhexanoate] Processed by Two-Step Drawing with Intermediate Annealing

Taizo Kabe,[1,2,3] Chizuru Hongo,[1,4] Toshihisa Tanaka,[2,5] Takaaki Hikima,[6] Masaki Takata,[2] Tadahisa Iwata[1,2,3]

[1]Department of Biomaterial Sciences, Graduate School of Agricultural and Life Sciences, The University of Tokyo, 1-1-1 Yayoi, Bunkyo-ku, Tokyo 113-8657, Japan

[2]Structural Materials Science Laboratory, RIKEN Harima Institute, SPring-8, 1-1-1 Kouto, Sayo-cho, Sayo-gun, Hyogo 679-5148, Japan

[3]Japan Science and Technology Agency, CREST, 4-1-8 Honcho, Kawaguchi, Saitama 332-0012, Japan

[4]Department of Chemical Science and Engineering, Graduate School of Engineering, Kobe University, 1-1 Rokko-cho, Nada-ku, Kobe-shi, Hyogo 657-8501, Japan

[5]Faculty of Textile Science and Technology, Shinshu University, 3-15-1 Tokida, Ueda, Nagano 386-8567, Japan

[6]Research Infrastructure Group, RIKEN Harima Institute/SPring-8 Center, 1-1-1 Kouto, Sayo-cho, Sayo-gun, Hyogo 679-5148, Japan

Correspondence to: T. Iwata (E-mail: atiwata@mail.ecc.u-tokyo.ac.jp)

ABSTRACT: High tensile strength fibers of poly[(*R*)-3-hydroxybutyrate-*co*-(*R*)-3-hydroxyhexanoate] [P(3HB-*co*-3HH)], a type of microbial polyesters, were processed by one-step and two-step cold-drawn method with intermediate annealing. Thermal degradation behaviors were characterized by differential scanning calorimeter and gel permeation chromatography measurements. Thermal analyses were revealed that molecular weights decreased drastically within melting time at a few minute. One-step cold-drawn fiber with drawing ratio of 10 showed tensile strength of 281 MPa, while tensile strength of as-spun fiber was 78 MPa. When two-step drawing was applied for P(3HB-*co*-3HH) fibers, the tensile strength was led to 420 MPa. Furthermore, the optimization of intermediate annealing condition leads to enhance the tensile strength at 552 MPa of P(3HB-*co*-3HH) fiber. Wide-angel X-ray diffraction measurements of these fibers suggest that the fibers with high tensile strength include much amount of the planer-zigzag conformation (β-form) as molecular conformation together with 2_1 helix conformation (α-form). © 2014 Wiley Periodicals, Inc. J. Appl. Polym. Sci. **2015**, *132*, 41258.

KEYWORDS: biodegradable; fibers; structure-property relations; thermal properties; X-ray

Received 26 March 2014; accepted 5 July 2014
DOI: 10.1002/app.41258

INTRODUCTION

Plastics are currently one of the most important materials for every life, whereas those include a significant problem of environmental pollution and stable supply. Eco-friendly polymers are expected to be put to practical use. Polyhydroxyalkanoate (PHA) that is a biodegradable polyester biosynthesized within microorganisms is called as the microbial polyester.[1–3] Poly[(*R*)-3-hydroxybutyrate] (P(3HB)) is the most famous microbial polyester in PHA family and it is well known as a brittle material and aging deterioration occurs due to the secondary crystallization at room temperature.[4,5] In recent year, the improvements for physical properties were reported by many researchers. Synthesis of ultrahigh-molecular-weight P(3HB),[6–8] development of novel drawing method,[9–16] biosynthesis of copolymerization[3,17–22] and blending[23,24] are such examples. The second monomer leads to be enhanced flexibility due to prevent for crystallization of P(3HB). Major second monomers on P(3HB) copolymer are (*R*)-3-hydroxyvalyrate (3HV),[25] (*R*)-3-hydroxyhexanoate (3HH)[20,22] and 4-hydroxybutyrate (4HB).[18] Among P(3HB) copolymers, the poly[(*R*)-3-hydroxybutyrate-*co*-(*R*)-3-hydroxyhexanoate] [P(3HB-*co*-3HH)] can be produced from palm oil.[26]

When P(3HB-*co*-3HH) is crystallized, the 3HH unit is excluded from the P(3HB) crystal.[22] Thus, 3HH unit leads to decrease melting point and crystallinity. However, thermal degradation temperature of P(3HB-*co*-3HH) is almost same as that of

P(3HB), suggesting that temperature range of melt-spinning is widen.[22,23,27] Until now, few study reported on preparation of the melt-spinning fiber of P(3HB-*co*-3HH).[28,29] Jikihara et al. have been reported P(3HB-*co*-3HH) fiber processed by one-step drawing method with tensile strength of 220 MPa.[30] It is well known that manufactural fibers such as bonded-fiber fabric need the tensile strength at 400–700 MPa. For this reason, it is necessary to improve the tensile strength of P(3HB-*co*-3HH) fiber.

By the way, tensile strength is very affected by molecular conformation and highly order structure. It is well known that the P(3HB) and its copolymers have two molecular conformations. One is 2_1 helix conformation (α-form)[31,32] which is universally observed in these materials, such as injection-moldings, films, and fibers. Another one is a planer-zigzag conformation (β-from)[33] which is only observed in drawn films or drawn fibers with high tensile strength.[12,34–36] While the generation mechanism of β-form structure has not been revealed, it is clear that the forming of β-form structure is important to make the high tensile strength fiber of P(3HB) copolymer. Some researchers expect that the β-form of P(3HB) chains is formed from tie-chains in amorphous region between lamellar crystals by stretching.[13,14,37] Thus, to form the β-form of P(3HB) chains, it is expected that two-step cold-drawing is optimal drawing method.

The purpose in this work is to achieve the high tensile strength at over 400 MPa of P(3HB-*co*-3HH) fiber. This work was performed to prepare the P(3HB-*co*-3HH) fiber with high tensile strength using two-step cold-drawing method with the intermediate annealing process Intermediate annealing process grows lamellar crystals, and tensile strength is expected to improve significantly by following drawing process against tie-chains between lamellar crystal, which produces β-form. Furthermore, the relationship between the amount of two kinds of molecular conformations of α-form and β-form and mechanical properties is revealed by synchrotron X-ray measurement.

EXPERIMENTAL

Materials

P(3HB-*co*-3HH) pellet with weight-average molecular-weight (M_w) = 5.5 × 10^5 and polydispersity (M_w/M_n) = 2.5 was supplied by Kaneka corporation. This P(3HB-*co*-3HH) includes 3HH unit as the second monomer at 5.5 mol %. The pellet was dried in vacuum at room temperature for 3 day before using.

Thermal Properties

The glass transition temperature (T_g) and melting temperature (T_m) were measured by differential scanning calorimeter (DSC) (Perkin-Elmer, DSC8500). Temperature calibration was performed using T_m of indium at 156.60°C. The first run was measured at 20°C/min from 40 to 180°C, maintained at 180°C for 1 min, and the cooled to −50°C at a rate of −200°C/min. After that, the second run was measured at 20°C/min from −20 to 180°C.

Molecular Weight Measurement During the Melt-Spun Process

The change of molecular weight during melt-spun process was measured to decide the melt-spinning conditions. The P(3HB-*co*-3HH) pellet was placed into the spinning apparatus at different temperatures of 170, 180, 190, or 200°C. The P(3HB-*co*-3HH) pellets were melted at different melting time from 1 to 10 min and then extruded from spinning apparatus. Melt-extruded samples were taken up for each 1 min, and then M_w and M_n were measured by gel permeation chromatography (Shimadzu, 10A series, Japan) at 40°C, which was equipped refractive detector with two joint colums of Shodex K-806M and K-802. Chloroform was used as the eluent at a flow rate of 0.8 mL/min. Polystyrene standards were used to make a molecular weight calibration curve.

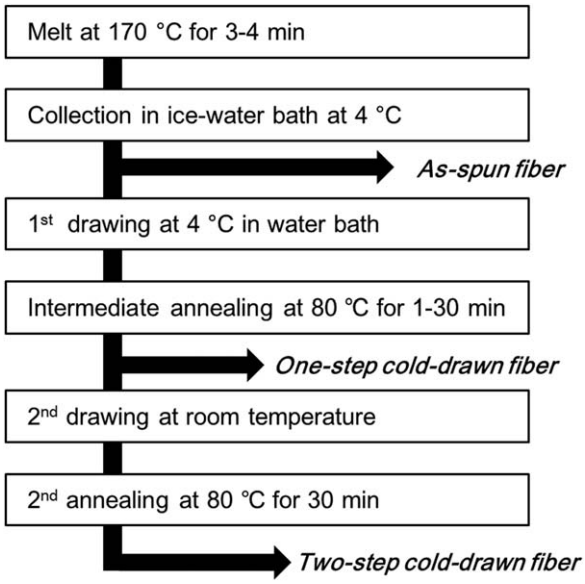

Figure 1. Experimental scheme to prepare fibers.

Preparation for P(3HB-*co*-3HH) Fiber by Melt-Spinning

Melt-spinning was carried out by melt-spinning apparatus (Imoto, 19F8, Japan). Melting temperature, melting time, die diameter, and volume velocity of extruded sample from die were chosen at 170°C, 3–4 min, 1 mm, and 4 mm^3/s. The as-spun fiber was collected at take-up of 70 m/min in ice water bath at 4°C. The following drawing methods were applied to collected molten state fiber method.

One- and Two-Step Cold-Drawing Method

The as-spun fiber was fixed on hand-made drawing machine in ice water bath at 4°C. And then, these fibers were stretched at drawing ratio (DR) of 4 or 8 in ice water bath, subsequently annealed at 80°C for 30 min in an oven. This cold-drawn and annealed drawn fiber is named an one-step cold-drawn fiber. One-step cold-drawn fibers were further stretched at room temperature, subsequently annealed at 80°C for 30 min in an oven. These two-step drawn and annealed fibers are named a two-step cold-drawn fiber. Experimental scheme is shown in Figure 1.

Effect of Intermediate Annealing on Two-Step Cold-Drawn Fibers

To investigate the influence of first annealing on two-step cold-drawn fibers, one-step cold-drawn fibers with first cold-DR of 8 were annealed for different annealing time (1–30 min) at 80°C. Drawing was performed at DR from 1.2 to 2.0.

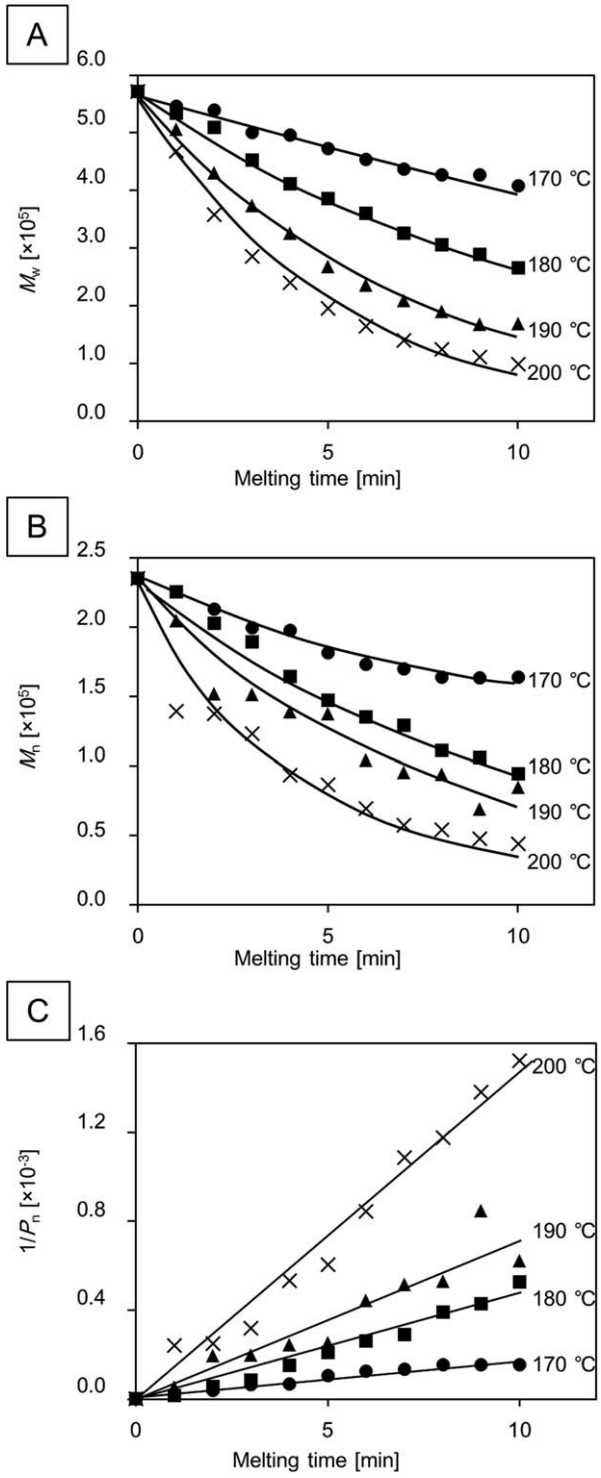

Figure 2. The relationship between melting time and (A) weight-average molecular weight, (B) number-average molecular weight, and (C) inverse average degree of polymerization at different melting temperature: (●)170°C; (■)180°C; (▲)190°C; (×)200°C.

Mechanical Properties

Mechanical properties of fibers prepared with different drawing method were measured by tensile testing machine (Shimadzu, EZ-test, Japan). The gauge length and crosshead speed were 10 mm and 20 mm/min, respectively. Fiber diameter was measured by optical microscope.

Molecular Chain Conformation Analysis

Fibers were analyzed to investigate the relationship between molecular conformation and mechanical properties by Wide-angle X-ray diffraction (WAXD) measurement. WAXD measurement was performed by synchrotron X-ray in SPring-8 at BL-45XU and BL-47XU, or laboratory scale X-ray. Wave length, camera length, and detector of synchrotron X-ray were set at 0.1 nm, 90 mm, and CCD camera, respectively. The laboratory scale X-ray measurement were carried out using Ni-filterd Cu Kα radiation of a wave length 0.15418 nm, from a rotating anode X-ray generator (Rigaku RU-200BH). Imaging plate was chosen as a detector.

RESULTS AND DISCUSSION

Thermal Properties of P(3HB-*co*-3HH)

Grass transition temperature (T_g) was detected at 2°C and two melting temperatures (T_ms) were observed at 121°C (T_{m1}) and 138°C (T_{m2}). T_{m1} and T_{m2} seem to be due to the melting of original crystals and melt-recrystallized crystals, respectively. Since thermal degradation temperatures of P(3HB-*co*-3HH) and P(3HB) are almost same as 220°C, and T_m of P(3HB-*co*-3HH) is lower than that of P(3HB) (ca.178°C), the spinnability of P(3HB-*co*-3HH) is better than that of P(3HB).

Thermal Degradation Behavior of P(3HB-*co*-3HH)

Figure 2 shows the relationship between melting time and molecular weights (M_w and M_n) at each melting temperature. In the case of the curves at melting temperatures over 180°C, the molecular weight drastically decreased. Especially, initial thermal degradation quickly progressed, for example, the M_w of curve at 200°C has become to half during melting for 3 min of melting time. The cause of drastically decreasing within a few minute is the random thermal degradation of molecular chains.[38,39] In the case of the curve at low melting temperature such as 170°C, thermal degradation relatively mildly progressed.

If the thermal degradation of the P(3HB-*co*-3HH) molecular chains occurs randomly, the number-average degree of polymerization ($P_{n,t}$) at time t is given by a reversible reaction with second-order kinetics [eq. (1)].[39,40]

Table I. Thermal Degradation Constants (K_d) of Each Sample at Four Temperatures (170, 180, 190, and 200°C), as Calculated from the Slope of Melt-Spinning Time Versus 1/P_n in Figure 2C

Melting temperature	Sample	
	P(3HB-*co*-3HH)	P(3HB)[40]
170°C	0.180×10^{-4} min^{-1}	-
180°C	0.464×10^{-4} min^{-1}	0.323×10^{-4} min^{-1}
190°C	0.716×10^{-4} min^{-1}	0.533×10^{-4} min^{-1}
200°C	1.470×10^{-4} min^{-1}	1.021×10^{-4} min^{-1}

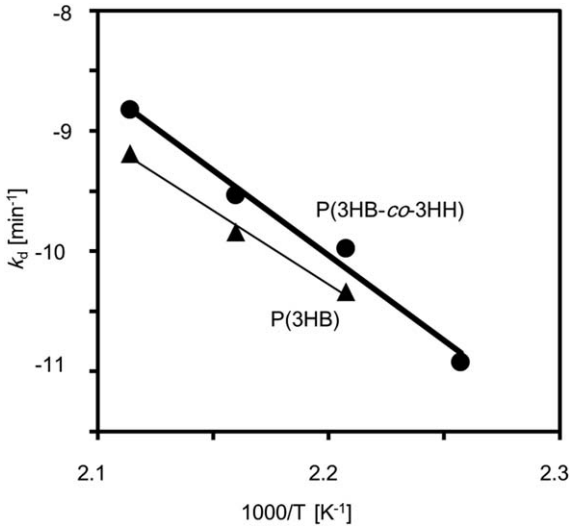

Figure 3. Arrhenius plot for the constants K_d of randomly chain scission for (●) P(3HB-*co*-3HH) and (▲) P(3HB),[40] respectively.

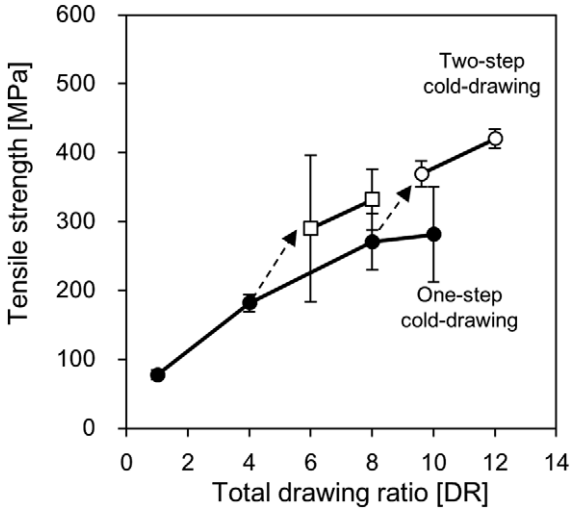

Figure 4. Tensile strength as a function of TDR. Three symbols indicate that (●) is one-step cold-drawn fiber from as-spun fiber: (□) is two-step cold-drawn fiber from one-step cold-drawn fiber with DR of 4: (○) is two-step cold-drawn fiber form cold-drawn fiber with DR of 8.

$$\frac{1}{P_{n,t}} = K_d t + \frac{1}{P_{n,0}} \quad (1)$$

Here, $P_{n,t}$ is average degree of polymerization at melting time after t min and $P_{n,0}$ is initial average degree of polymerization. Inverse average degree of polymerization, which is calculated from M_n, is plotted as a function of melting time in Figure 2(C). Thermal degradation mode of P(3HB-*co*-3HB) seems to be randomly since the plotted points in Figure 2(C) have linearity. The thermal degradation constants (K_d) are calculated from the slope of these lines are listed in Table I. The large value of K_d indicates the easily progress of thermal degradation. The calculated K_d value of P(3HB-*co*-3HH) at each temperature is smaller than that of P(3HB).[40] The K_d values of another P(3HB) copolymers, such as poly[(*R*)-3-hydroxybutyrate-*co*-(*R*)-3-hydroxyvalyrate] (P(3HB-*co*-3HV)) and poly[(*R*)-3-hydroxybutyrate-*co*-4-hydroxybutyrate](P(3HB-*co*-4HB)), are also reported to be smaller than that of P(3HB) by Kunioka and Doi.[39] Thus, P(3HB-*co*-3HH) is also degraded later than P(3HB) as same as other P(3HB) copolymers.

The logarithm of constant K_d at each melting temperature is plotted against inverse temperature in Figure 3. The activation energy (E_a) was calculated from the slop of line in Figure 3. The large value of E_a means high resistance for thermal degradation. The E_a values of P(3HB-*co*-3HH) and P(3HB) were calculated as 118 and 102 kJ/mol, respectively, and these values are very close. This result and low melting temperature of P(3HB-co-3HH) also indicate the wide working temperature range of P(3HB-*co*-3HH) compared with P(3HB).

Melt-Spinning of P(3HB-*co*-3HH) Fiber

The molten state conditions of P(3HB-*co*-3HH) were observed at different melting temperature and melting time to be able to spin the fiber. Immediately after heating at all melting temperatures, it was difficult to spin the fibers because the molten P(3HB-*co*-3HH) remained hard and brittle, indicating that the polymers did not completely melt. When the longer melt-spinning time was applied, continuous spinning was enable because of the low melt viscosity of the molten samples by

Table II. Mechanical Properties of One-Step and Two-Step Cold-Drawn Fibers

Specimen	1st drawing ratio	2nd drawing ratio	Total drawing ratio (TDR)	Tensile strength (MPa)	Elongation at break (%)	Young's modulus (GPa)
One-step cold-drawn fiber	1	-	1	78 ± 7	821 ± 75	0.91 ± 0.35
	4	-	4	182 ± 12	222 ± 43	0.93 ± 0.37
	8	-	8	271 ± 41	62 ± 17	1.58 ± 0.48
	10	-	10	281 ± 69	78 ± 32	1.40 ± 0.36
Two-step cold-drawn fiber	4	1.5	6	290 ± 6	81 ± 66	1.67 ± 0.90
	4	2.0	8	332 ± 44	46 ± 28	1.91 ± 0.48
	8	1.2	9.6	369 ± 19	42 ± 19	2.34 ± 0.13
	8	1.5	12	420 ± 14	38 ± 6	2.13 ± 0.44

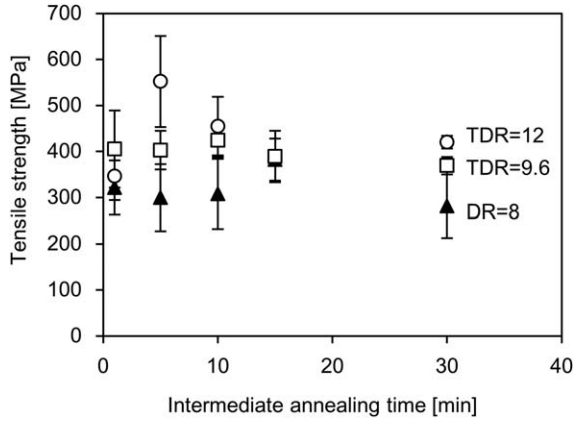

Figure 5. Tensile strength as a function of intermediate annealing time. DR = 8 indicate one-step cold-drawn fiber with DR of 8 (▲). TDR=9.6 (□) and TDR = 12 (○) indicate two-step cold-drawn fibers with TDR of 9.6 (8 × 1.2) and 12 (8 × 1.5), respectively.

thermal degradation. Melting temperature and melting time was chosen at 170°C and 3–4 min, respectively, because that the reduction of molecular weight was the smallest in spinnable melting conditions.

One-Step and Two-Step Cold-Drawn Fibers

Tensile strength, elongation at break and Young's modulus of as-spun, one-step cold-drawn, and two-step cold-drawn fibers are listed in Table II, and tensile strength was plotted as a function of one-step drawing rate in Figure 4. Tensile strength of one-step cold-drawn fibers increased with increasing the one-step cold-DR, while the tensile strength of as-spun fiber shows 78 MPa. The maximum value of tensile strength in one-step cold-drawn fiber was shown 281 MPa at maximum DR of 10. Tensile strengths of two-step cold-drawn fibers are also plotted in Figure 4. The abscissa axis of Figure 4 indicates the total drawing ratio (TDR) which is multiplication of one-step and two-step cold-DR. The one-step cold-drawn fibers with one-step cold-DR of 4 or 8 were able to draw furthermore until at two-step cold-DR of 2.0 (TDR = 4 × 2 = 8) or 1.5 (TDR= 8 × 1.5 = 12). The tensile strength of two-step cold-drawn fiber at TDR of 8 was higher than those of one-step cold-drawn fiber with one-step drawn ratio of 8, which means two-step cold-drawing has much effect on the improvement of tensile strength of P(3HB-*co*-3HH) fibers. The tensile strength of two-step cold-drawn fibers with at TDR of 12(8 × 1.5) was achieved to be the highest value of 420 MPa.

Optimization of Intermediate Annealing Time on Two-Step Cold-Drawn Fibers

In this section, the two-step cold-drawn fibers with different intermediate annealing time were investigated to understand the influence of intermediate annealing time. Three types of fibers, one-step cold-drawn fibers with DR of 8, two-step cold-drawn fibers at TDR of 9.6 (8 × 1.2) and 12 (8 × 1.5), were prepared with different intermediate annealing time of 1, 5, 10, 15, and 30 min. Figure 5 shows the tensile strength of three types of fibers as a function of intermediate annealing time, and the tensile strength, elongation at break and Young's modulus of fibers were listed in Table III. The tensile strengths of one-step cold-drawn fiber with DR = 8 show about 300 MPa regardless intermediate annealing time. The tensile strengths (400 MPa) of two-step cold-drawn fibers at TDR = 9.6 (8 × 1.2) show maximum value at intermediate annealing time of 10 min. And, tensile strength of two-step cold-drawn fiber with TDR = 12 (8 × 1.5) had the maximum value when intermediate annealing time was 5 min. This maximum tensile strength is 552 MPa which is the highest value in reported P(3HB-*co*-3HH) fibers by our knowledge. Thus, 5 min of intermediate annealing time is

Table III. Mechanical Properties of One-Step and Two-Step Cold-Drawn Fibers with Different Intermediate Annealing Time

Specimen	Annealing Time (min)	Tensile strength (MPa)	Elongation at break (%)	Young's modulus (GPa)
One-step cold-drawn fiber at drawing ratio of 8	1	322 ± 69	63 ± 23	2.81 ± 0.91
	5	300 ± 72	70 ± 15	2.75 ± 0.53
	10	308 ± 76	37 ± 16	1.88 ± 0.07
	15	383 ± 46	70 ± 15	2.25 ± 0.76
	30	281 ± 69	78 ± 32	1.40 ± 0.36
Two-step cold-drawn fiber at total drawing ratio of 9.6 (8 × 1.2)	1	406 ± 84	59 ± 20	2.24 ± 1.08
	5	403 ± 42	60 ± 9	2.60 ± 0.66
	10	425 ± 37	43 ± 4	2.87 ± 0.44
	15	389 ± 56	40 ± 8	2.23 ± 0.96
	30	369 ± 19	42 ± 19	2.34 ± 0.13
Two-step cold-drawn fiber at total drawing ratio of 12 (8 × 1.5)	1	346 ± 51	85 ± 54	2.26 ± 0.71
	5	552 ± 99	48 ± 22	3.76 ± 1.38
	10	455 ± 64	39 ± 11	3.13 ± 0.61
	30	420 ± 14	38 ± 6	2.13 ± 0.44

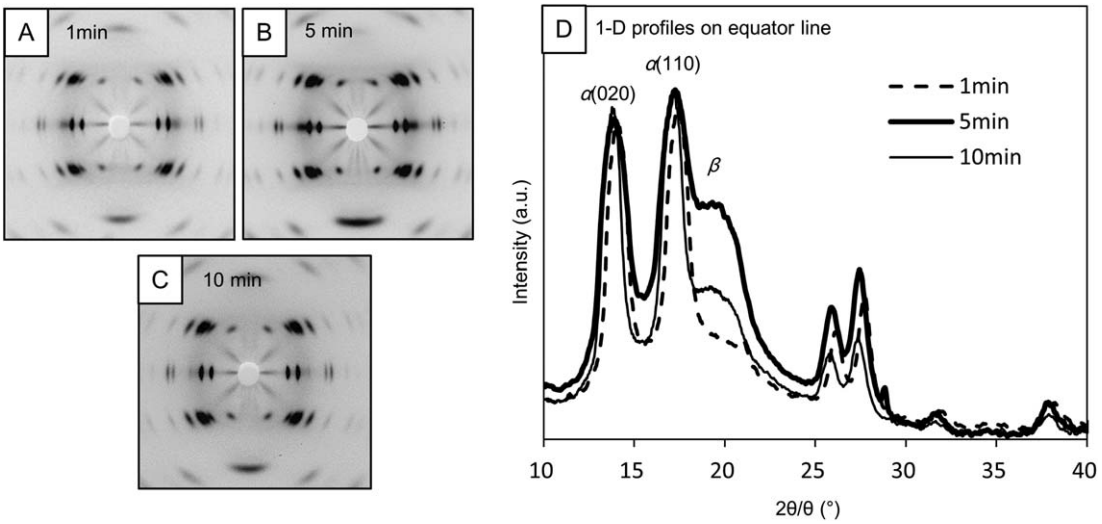

Figure 6. The two-dimensional WAXD patterns of two-step cold-drawn fiber with intermediate annealing at (A) 1 min, (B) 5 min, and (C) 10 min. (D) one-dimensional profiles on equator line of A, B, and C.

enough to increase the tensile strength of two-step cold-drawn fiber. The appearance of the maximum value with changing intermediate annealing time probably concerns an amount of formed β-form. Our group has reported the positive correlation between tensile strength and the amount of β-form in previous report.[35] In the case of two-step cold-drawn fiber with TDR = 12, it is seemed that the short intermediate annealing time at 1 min formed a little tie-chain due to low crystallinity,

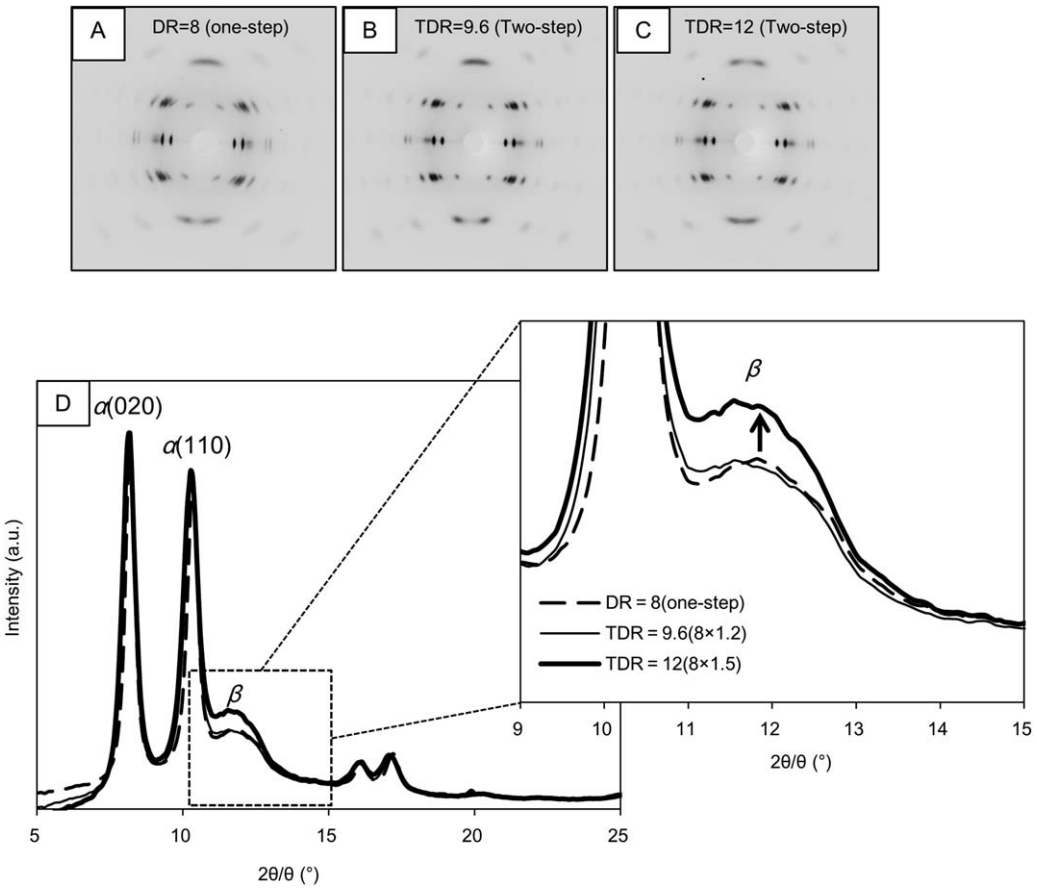

Figure 7. WAXD diagrams of one-step cold-drawn fibers with DR = 8 (A), two-step cold-drawn fibers with TDR=9.6 (B), and TDR=12 (C). Intermediate annealing time of all fibers is 5 min. (D) The profiles on equator line were obtained fiber WAXD diagrams of A, B, and C.

thus the amount of β-form is formed less. However, the long intermediate annealing time from 10 to 30 min lead to grow the lamellar crystals, and high crystallinity induces decreasing of formed tie-chain and following formation of β-form from tie-chain. The different intermediate annealing time of maximum tensile strength between TDR = 9.6 and 12 suggests that the optimum intermediate annealing time is different depending to TDR.

Wide-Angle X-ray Diffraction

To investigate the relationship between annealing time and the amount of β-form structure, WAXD measurements were carried out for the two-step cold-drawn fiber with different annealing time at 1, 5, and 10 min by laboratory scale X-ray, which shown in Figure 6(A–C). Figure 6(D) shows the equator line profiles obtained from these WAXD patterns. All equator line profiles were standardize by the intensity of diffraction from α(020). The amount of β-form structure of two-step cold-drawn fiber with annealing time at 5 min is the largest value. This result supports the mechanical properties of two-step cold-drawn fiber with different intermediate annealing time.

Figure 7(A–C) shows the WAXD patterns of one-step cold-drawn fiber at DR = 8, two-step cold-drawn fiber at TDR = 9.6 (8 × 1.2) and at TDR = 12 (8 × 1.5), respectively. The intermediate annealing time of these fibers are 5 min. These WAXD patterns were obtained using synchrotron X-ray. When compared the line profiles data, the intensity of β-form of two-step cold-drawn film with TDR = 12 is very strong. Thus, it is probable that a large segment of β-form structure was formed by two-step cold-drawing at TDR between 9.6 and 12. The difference in amount of β-form structure between DR = 8 and TDR = 9.6 is small compared with difference between TDR = 9.6 and TDR = 12, despite the difference in tensile strengths of TDR = 9.6 and TDR = 12 is large. These results would yield that the strengthening mechanism of above or until TDR = 9.6 is different. In the case of TDR until 9.6, the strengthening mechanism is mainly caused by molecular chain orientation. Conversely, in the case of high TDR as TDR 12, the strengthening mechanism includes the influence of formed β-form structure.[35]

CONCLUSIONS

In this article, we investigate the thermal degradation of P(3HB-*co*-3HH) during isothermal melting for melt-spinning. And then, to prepare the P(3HB-*co*-3HH) fibers with high tensile strength, we have attempted to apply two-step cold-drawing method with intermediate annealing process. The melt-spinning condition was chosen the melting temperature at 170°C and the melting time for 3-4 min based on results which are analysis for thermal properties and the measurement of thermal degradation behavior. When applied one-step cold-drawing method for P(3HB-*co*-3HH) fiber, the tensile strength of P(3HB-*co*-3HH) fiber was improved from 78 MPa (as-spun) to 281 MPa (one-step cold-drawing method at DR = 10). Furthermore, two-step cold-drawing method with intermediate annealing process increased the tensile strength of P(3HB-*co*-3HH) fiber until 552 MPa. These results show that the two-step cold-drawing with intermediate annealing process is effective for improvement in tensile strength of P(3HB-*co*-3HH) fiber. The WAXD measurement revealed that the P(3HB-*co*-3HH) fiber with high tensile strength includes a lot of β-form structure.

ACKNOWLEDGMENTS

This work was partially supported by a Grant-in-Aid for Scientific Research of Japan (A) No.22245026 (2010), the New Energy and Industrial Technology Development Organization (NEDO) of Japan, the society of fiber science and technology, Japan and JST, CREST. Synchrotron radiation experiments were performed at BL45XU of SPring-8 with the approval of RIKEN, and BL47XU of SPring-8 with the approval of the Japan Synchrotron Radiation Research Institute (JASRI) (Proposal No. 2011B1711).

REFERENCES

1. Macrae, R. M.; Wilkinson, J. F. *J. Gen. Microbiol.* **1958**, *19*, 210.
2. Lenz, R. W.; Marchessault, R. H. *Biomacromolecules* **2005**, *6*, 1.
3. Sudesh, K.; Abe, H.; Doi, Y. *Prog. Polym. Sci.* **2000**, *25*, 1503.
4. Scandola, M.; Ceccorulli, G.; Pizzoli, M. *Makromol. Chem. Rapid Commun.* **1989**, *10*, 47.
5. deKoning, G. J. M.; Kellerhals, M.; vanMeurs, C.; Witholt, B. *Bioprocess. Eng.* **1997**, *17*, 15.
6. Kusaka, S.; Abe, H.; Lee, S. Y.; Doi, Y. *Appl. Microbiol. Biotechnol.* **1997**, *47*, 140.
7. Kusaka, S.; Iwata, T.; Doi, Y. *J. Macromol. Sci. Pure Appl. Chem.* **1998**, *35*, 319.
8. Agus, J.; Kahar, P.; Abe, H.; Doi, Y.; Tsuge, T. *Polym. Degrad. Stab.* **2006**, *91*, 1138.
9. Furuhashi, Y.; Imamura, Y.; Jikihara, Y.; Yamane, H. *Polymer* **2004**, *45*, 5703.
10. Iwata, T.; Tsunoda, K.; Aoyagi, Y.; Kusaka, S.; Yonezawa, N.; Doi, Y. *Polym. Degrad. Stab.* **2003**, *79*, 217.
11. Iwata, T.; Aoyagi, Y.; Fujita, M.; Yamane, H.; Doi, Y.; Suzuki, Y.; Takeuchi, A.; Uesugi, K. *Macromol. Rapid Commun.* **2004**, *25*, 1100.
12. Iwata, T. *Macromol. Biosci.* **2005**, *5*, 689.
13. Tanaka, T.; Fujita, M.; Takeuchi, A.; Suzuki, Y.; Uesugi, K.; Ito, K.; Fujisawa, T.; Doi, Y.; Iwata, T. *Macromolecules* **2006**, *39*, 2940.
14. Tanaka, T.; Yabe, T.; Teramachi, S.; Iwata, T. *Polym. Degrad. Stab.* **2007**, *92*, 1016.
15. Yamane, H.; Terao, K.; Hiki, S.; Kimura, Y. *Polymer* **2001**, *42*, 3241.
16. Kabe, T.; Tanaka, T.; Kasuya, K.; Ito, K.; Takata, M.; Takemura, A.; Iwata, T. *Sen'i Gakkaishi 66*, 253, **2010**.
17. Bloembergen, S.; Holden, D. A.; Hamer, G. K.; Bluhm, T. L.; Marchessault, R. H. *Macromolecules* **1986**, *19*, 2865.
18. Doi, Y.; Kunioka, M.; Nakamura, Y.; Soga, K. *Macromolecules* **1988**, *21*, 2722.
19. Hiramitsu, M.; Doi, Y. *Polymer* **1993**, *34*, 4782.

20. Liebergesell, M.; Mayer, F.; Steinbuchel, A. *Appl. Microbiol. Biotechnol.* **1993**, *40*, 292.
21. Kichise, T.; Fukui, T.; Yoshida, Y.; Doi, Y. *Int. J. Biol. Macromol.* **1999**, *25*, 69.
22. Doi, Y.; Kitamura, S.; Abe, H. *Macromolecules* **1995**, *28*, 4822.
23. Feng, L. D.; Watanabe, T.; He, Y.; Wang, Y.; Kichise, T.; Fukuchi, T.; Chen, G. Q.; Doi, Y.; Inoue, Y. *Macromol. Biosci.* **2003**, *3*, 310.
24. Kabe, T.; Sato, T.; Kasuya, K.-i.; Hikima, T.; Takata, M.; Iwata, T. *Polymer* **2014**, *55*, 271.
25. Holmes, P. A. *Phys. Technol.* **1985**, *16*, 32.
26. Loo, C. Y.; Lee, W. H.; Tsuge, T.; Doi, Y.; Sudesh, K. *Biotechnol. Lett.* **2005**, *27*, 1405.
27. Watanabe, T.; He, Y.; Fukuchi, T.; Inoue, Y. *Macromol. Biosci.* **2001**, *1*, 75.
28. Bond, E. B. *Macromol. Symp.* **2003**, *197*, 19.
29. Zini, E.; Focarete, M. L.; Noda, I.; Scandola, M. *Compos. Sci. Technol.* **2007**, *67*, 2085.
30. Jikihara, Y.; Saito, T.; Yamane, H. *Sen'i Gakkaishi* **2006**, *62*, 115.
31. Okamura, K.; Marchessault, R. H. In Conformation of Biopolymers; Ramachandran G. N., Ed.; Academic Press: London, **1967**, Chapter 2.
32. Yokouchi, M.; Chatani, Y.; Tadokoro, H.; Teranish. K.; Tani, H. *Polymer* **1973**, *14*, 267.
33. Orts, W. J.; Marchessault, R. H.; Bluhm, T. L.; Hamer, G. K. *Macromolecules* **1990**, *23*, 5368.
34. Iwata, T.; Aoyagi, Y.; Tanaka, T.; Fujita, M.; Takeuchi, A.; Suzuki, Y.; Uesugi, K. *Macromolecules* **2006**, *39*, 5789.
35. Kabe, T.; Tsuge, T.; Kasuya, K.; Takemura, A.; Hikima, T.; Takata, M.; Iwata, T. *Macromolecules* **2012**, *45*, 1858.
36. Zhang, J. Q.; Kasuya, K.; Hikima, T.; Takata, M.; Takemura, A.; Iwata, T. *Polym. Degrad. Stab.* **2011**, *96*, 2130.
37. Iwata, T.; Fujita, M.; Aoyagi, Y.; Doi, Y.; Fujisawa, T. *Biomacromolecules* **2005**, *6*, 1803.
38. Kim, K. J.; Doi, Y.; Abe, H. *Polym. Degrad. Stab.* **2006**, *91*, 769.
39. Kunioka, M.; Doi, Y. *Macromolecules* **1990**, *23*, 1933.
40. Kabe, T.; Tsuge, T.; Hikima, T.; Takata, M.; Takemura, A.; Iwata, T. In Biobased Monomers, Polymers, and Materials; Patrick B. S. and Richard A. G., Eds.; American Chemical Society, **2012**, Chapter 5. Washington, DC.